



Combining Isotopic Techniques to Assess Historical Sediment Delivery in a Forest Catchment in Central Chile

C. Bravo-Linares¹ · P. Schuller¹ · A. Castillo¹ · A. Salinas-Curinao¹ · L. Ovando-Fuentealba¹ · E. Muñoz-Arcos¹ · A. Swales² · M. Gibbs² · G. Dercon³

Received: 6 June 2019 / Accepted: 16 September 2019 / Published online: 22 October 2019
© Sociedad Chilena de la Ciencia del Suelo 2019

Abstract

The purpose of this research was to determine the historical evolution of different sources of sediment by land uses in a forest catchment, through the combination of two isotopic techniques: (i) fallout radionuclides (FRNs) for dating sediment cores and (ii) compound-specific stable isotope (CSSI). Ten 30-cm-deep sediment cores (taken in a meander at the outlet of the forest catchment) were used to reconstruct the sediment delivery history for around 67 years before present (BP), i.e., 2012. Five land uses were considered as potential sources in this analysis: forest roads, pine trees, eucalyptus trees, native forest (buffer or riparian zone), and wheat. Forestry activities incremented the sedimentation rate by about 17% compared to wheat production. Results were consistent with the historical land uses in the catchment. The analysis showed an important sediment contribution of farmland used for wheat from 1945 to about 1974 (~20–80%). After the implementation of the public bill, the sediment source changed into the exotic plantations (pine and eucalyptus trees) until present, where harvesting periods were clearly seen as an increment of sediment delivery from the source.

Keywords Fatty acids · $^{210}\text{Pb}_{\text{ex}}$ · CSSIAR · Sediment fingerprinting · CSSI · Historical contribution

1 Introduction

The progressive clearance of native forest to grow wheat in central Chile (from the mid-eighteenth century to the early twentieth century) caused severe degradation of soil, water resources and the landscape (Gysling et al. 2016). Wheat cultivation was the main agricultural activity until mid-twentieth century (Brunel et al. 2013). These agricultural practices caused severe deterioration of land productivity mainly due to gully erosion. Between 1940 and 1950, several investigations were conducted to evaluate the severity and the effects of

soil erosion in the Central Chile region. These studies suggested that production forestry would reduce soil erosion and generate a more suitable land use for these low-fertility soils. The tree species selected for production forestry were *Pinus radiata* and *Eucalyptus globulus*, being fast-growing species that could grow in low-fertility soils. The Chilean Government approved a public bill (No. 701) in 1974 that promoted the establishment of these degraded lands for forestry production. About 1.2 million ha of forest were planted during the first 20 years, and this increased to 2 million ha by the late 1990s. Currently, about 23% of the total land area of Chile is forested, of which 85% is native forest and 15% is forestry production (Gysling et al. 2016).

The production forestry sector has become one of main economic activities in Chile. Despite the original motivation to reduce soil erosion, particularly in steep-land catchments, this production forestry has led to a significant increase in soil erosion and sediment loads to receiving water bodies. These adverse effects largely coincide with road construction and the use of heavy machinery and clear-cut harvesting (Schuller et al. 2013).

Conventional techniques (e.g., GIS techniques, erosion pins, erosion plots) have been used by Chilean

✉ C. Bravo-Linares
cbravo@uach.cl

¹ Facultad de Ciencias, Instituto de Ciencias Químicas, Universidad Austral de Chile, Independencia, 641 Valdivia, Chile

² National Institute of Water and Atmospheric Research (NIWA), Hamilton, New Zealand

³ Soil and Water Management & Crop Nutrition Laboratory, Joint FAO/IAEA Division of Nuclear Techniques in Food and Agriculture, Department of Nuclear Sciences and Applications, International Atomic Energy Agency, Vienna, Austria

land management agencies to identify soil erosion hotspots in the landscape, including geographical information system (Bonilla et al. 2010) and other conventional techniques such as sediment traps (Tolorza et al. 2014; Pepin et al. 2010). Nowadays, these conventional techniques are being complemented by isotopic techniques, which are becoming more accessible and affordable tools to evaluate spatial and temporal patterns of soil erosion in the landscape (Brandt et al. 2018a; Mabit et al. 2018; Upadhayay et al. 2017; Smith and Blake 2014; Schuller et al. 2013). These isotopic techniques are particularly useful for identifying soil erosion hotspots. Fallout radionuclides (FRNs), including beryllium-7 (^7Be), caesium-137 (^{137}Cs), and excess lead-210 ($^{210}\text{Pb}_{\text{ex}}$), have been widely used as tracers to estimate soil erosion and deposition rates at multiple spatial and temporal scales at limited cost and without major time investment (Smith and Blake 2014; Dercon et al. 2012; Mabit et al. 2013; Taylor et al. 2013). Complementary, compound-specific stable isotope (CSSI) analysis of soils and sediments has emerged as a very useful technique to trace the sources and fate of eroded soils in the landscape (Mabit et al. 2018; Blake et al. 2012; Gibbs 2008). The CSSI sediment tracing method can be applied to a number of biomarkers (fatty acids, *n*-alkanes, etc.) and different isotopes ($\delta^{13}\text{C}$ and/or $\delta^2\text{H}$) (Bravo-Linares et al. 2018; Brandt et al. 2018a; Mabit et al. 2018; Upadhayay et al. 2017; Cooper et al. 2015). The CSSI sediment tracing technique can also be used to reconstruct changes in the contributions of land use sources from sedimentary records by correcting the $\delta^{13}\text{C}$ isotopic values of the fatty acid biomarkers for the Suess effect. The Suess effect accounts the depletion of the $\delta^{13}\text{C}$ values of atmospheric carbon dioxide due to burning of fossil fuels and the subsequent uptake by plants (Verburg 2007).

Previous studies have determined that the CSSI technique using $\delta^{13}\text{C}$ of fatty acids was able to discriminate different types of land use including forested catchments (Bravo-Linares et al. 2018; Brandt et al. 2018b). However, the reconstruction of historical land uses using combined isotopic techniques has not previously been applied in a production forestry catchment and only in a tropical agricultural catchment (Brandt et al. 2018b). Consequently, the main aim of our study is to evaluate how the combined use of CSSI and FRN can assist to reconstruct sedimentary records and how historical land use changes in a production forestry catchment has influenced soil erosion and land degradation over time. We hypothesize that both techniques and the historical antecedents of the land uses in the catchment will correspond each other, making the combined approach a feasible tool to evaluate sediment redistribution in a historical prospective, especially when the historical uses of a catchment are not available or well known.

2 Material and Methods

2.1 Study Site

The study site is the Nacimiento catchment, which is situated in the Bio-Bio Region, some 36 km west of Los Angeles city (south-central Chile, Fig. 1). The catchment has the following characteristics: annual mean precipitation of 1200 mm, surface of 12.7 ha, mean altitude (m a.s.l.) of 328 m, mean slope 19%, ~ 1 km of length of the main stream and no more than 2 m in the widest part, 0.3 km of road length and 33% of slopes, annual mean sediment yield of 600 kg ha⁻¹—under no harvest condition and mature forest (Schuller et al. 2013)—a climate temperate semi-oceanic and the main soil type (WRB) is Vitric Andosol.

The land use history of this catchment since the early 1960s is summarized in Table 1. Five potential historical and contemporary sources of eroded soils were identified from this record: unpaved forest roads, native forest (buffer or riparian zones), eucalyptus plantations, pine plantations, and wheat. With the exception of wheat (which is no longer grown in the region), soil samples to develop a source library for modeling were collected from the study site (Nacimiento catchment). The CSSI isotopic fatty acid composition for wheat was obtained from the National Institute of Water and Atmospheric Research (NIWA, New Zealand) from a soil sample that had the wheat planted in Chile (winter wheat) and collected in a similar latitude to the study site. Previous research demonstrated (unpublished results) that isotopic composition for other land uses within Chile and New Zealand were similar because they have common species grown in both countries (e.g., pine, eucalyptus).

In all other respects, the catchment represents the typical land uses that were implemented, as previously described in Chile, during the last 50 years.

2.2 Sample Collection

For CSSI source sampling, 13 samples were collected. Samples of topsoils (~ 2 cm) were collected from each land use from different parts of the catchment (4 samples of pine, 3 samples of buffer zone, 3 samples of road, and 3 samples of eucalyptus). Before sampling, the litter on the surface was removed with metal spatulas. Each source sample was generated from 5 composite samples taken at the corners and center of a 10 × 10 square, then were placed in a metal bucket and mixed, a subsample of ~ 1 kg was taken into the lab in double plastic bags for further analysis (Bravo-Linares et al. 2018).

For mixtures, ten replicates of core samples for CSSI and FRN techniques were taken in 2012 in 5-cm-diameter PVC core liners to 30-cm depth in the substrate. The core site was 30 m downstream from the end of the catchment, in an area where a meander was formed and in the border of the main

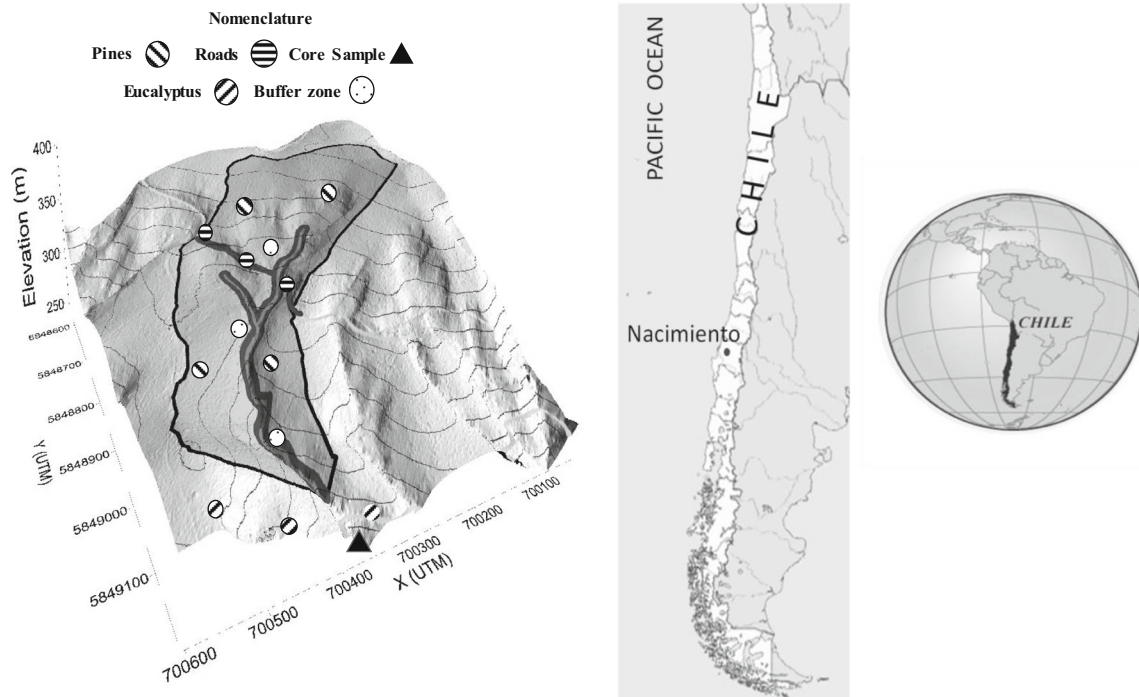


Fig. 1 Location of studied forest catchment in south-central Chile: Nacimiento (37° 29' S, 72° 44' W)

stream channel. The distance between each core sample was < 10 cm. Sediments were removed from the PVC tubes and placed in aluminum trays, where they were sliced into 2-cm-thick sections. The 2-cm-thick slices from each depth in each core were combined into a bulk sample, which was mixed and treated as a single sample for different analysis. Samples were composite to provide sufficient material for analysis (< 63 μ fraction) for FRN, CSSI, and other analyses (bulk δ¹³C, %C, δ¹⁵N, and %N).

2.3 Sample Preparation and Analysis

2.3.1 CSSI Analysis

Samples for sources (13) and for the final mixture (15 core combined slices) were oven dried at 60 °C, then first sieved through a 2.0 mm mesh and finally through a 63-μm sieve. The fatty acids were extracted from 20 g of dry soil samples using an accelerated solvent extractor (Dionex ASE 200) and dichloromethane (DCM) as the extraction solvent. The

samples were heated to 100 °C and raised to a pressure of 2000 psi for 10 min; this extraction procedure was repeated twice. The extracts were concentrated using a rotary evaporator at 35 °C and then taken to dryness under stream of oxygen-free dry nitrogen. Fatty acids were converted to their methyl esters (FAMES) by methylating the dry extract with 5% BF₃ catalyst in pure methanol solution and heating for 20 min at 70 °C (Bravo-Linares et al. 2018).

The δ¹³C isotopic values of the resulting FAMES (δ¹³C-FA) were determined using gas chromatography-combustion-isotope ratio mass spectrometry (GC-c-IRMS). The chromatographic conditions were as follows: column BP-5 (SGE), 30 m, 0.25 mm O.D., 0.25 mm film; constant flow 1.4 mL/min. The injector temperature was 280 °C; splitless (1 min). The instrument used was Agilent 6890 GC gas chromatograph coupled to a Thermo MAT 253 through a GC-C-III combustion interface. Combustion was done at 950 °C with NiO/CuO catalyst and reduction at 650 °C with Cu. The temperature program was as follows: 110 °C (hold 1 min); 220 °C (4 °C/min); 290 °C (10 °C/min, hold 10 min).

Table 1 Historical land use history of the Nacimiento catchment (1960–2020)

Time period*	Historical land use
2020	Expected year of harvesting
1986–1987	Harvesting and 2nd <i>Pinus radiata</i> planting
1974	Executive order N° 701 that promoted forestry plantations
1960–1974	1st <i>Pinus radiata</i> planting
?–1970	Wheat plantation

*Estimated dates provided by the forestry company Mininco

The isotopic results were methanol corrected to allow for the isotopic signature of the methyl radical added during methylation. The following equation was used (Gibbs 2008):

$$\delta^{13}C = \frac{\delta^{13}C_{FAMES} - (1-X)\delta^{13}C_{Methanol}}{X} \quad (1)$$

where X is calculated using the total number of carbons of the original fatty acid divided by the number of carbons of the derivatized molecule (FAME).

A further correction was made for the Suess effect based on the core slice dating from the FRN analysis of the core (further details are shown later). These $\delta^{13}C$ -FA data were then deconstructed into their source components using the mixing model CSSIAR V2.0 (de los Santos-Villalobos et al. 2017) applying the contemporary land use sources as the reference library. The resulting isotopic proportions were converted to soil proportions using a linear scaling equation and the %C content as a proxy (Gibbs 2008).

2.3.2 FRN Measurements

The core slices were oven dried at 60 °C for 4 days and disaggregated, then sieved through a 63 μ m sieve. An aliquot of ca. 80 g of each sample was sealed in a Petri dish and stored for 3 weeks prior to radiometric assay using an ORTEC high-resolution, extended range Ge detector of 53% relative efficiency. Count times were in excess of 72,000 s per sample, providing results with analytical precision of ca. 10% at the 95% level of confidence. The efficiency of the detector system was assessed using standard samples prepared by adding known quantities of mixed reference solutions provided by Eckert & Ziegler Nuclitec GmbH (type QCYB400 for the 46–122 keV energy range and type QCYB410 for the 122–1836 keV range). The total ^{210}Pb activity of the samples was measured at 46.5 keV, and the ^{226}Ra activity was obtained by measuring the activity of ^{214}Pb at 351.9 keV. The in situ ^{226}Ra supported ^{210}Pb concentration was derived from the measured ^{226}Ra concentration, using a reduction factor of 0.8 observed for samples collected in Nacimiento catchment. This reduction factor accounts for the loss of ^{222}Rn from the soil by fugacity to the atmosphere with the result that ^{210}Pb might not be in equilibrium with ^{226}Ra . The $^{210}Pb_{ex}$ concentration associated with a sample was calculated by subtracting the ^{226}Ra -supported ^{210}Pb concentration from the total ^{210}Pb concentration. Further details of the analysis are described in the literature (Schuller et al. 2013).

2.3.3 Complementary Analyses for Core Samples and QA/QC Protocols

Further analyses were done with the fractions used for CSSI and FRN analysis. Carbon and nitrogen percentages as well

bulk $\delta^{13}C$ and $\delta^{15}N$ were measured on a Delta Plus/Delta V plus after combustion in a NA 1500/Flash 2000 Elemental Analyser. For carbon, the carbonates were eliminated by adding 10% chlorhydric acid solution to the soil samples (this procedure was done twice, then samples were centrifuged and dried) prior to analysis in order to only consider the organic fraction.

Quality assurance and quality control (QA/QC) procedures were applied to different stages of this research. For the $\delta^{13}C$ of FAMES, average standard deviations of reference replicate measurements no greater than ± 0.5 across FAMES were acceptable. Internal standard of C12:0 and a reference mixture were added to each sample. Additionally, two reference mixtures (containing pure FAMES of calibrated $\delta^{13}C$) were co-analyzed with the samples. Additional FAME mixtures were analyzed to confirm retention times.

The mixing model employed was validated using artificial mixtures. This was done by generating artificially made mixture of the same land uses in this study and mixed artificially in known proportions. This provided a good validation of the mixing model used, concerning the ability to deconstruct known values (%) of artificial mixtures. The results of this analysis are presented in Bravo-Linares et al. (2018).

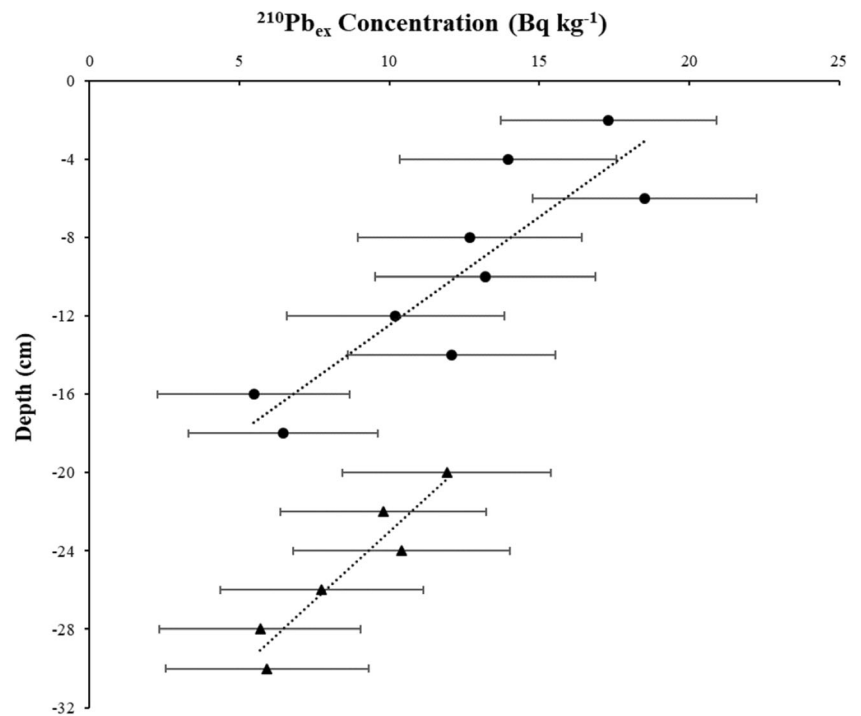
The $\delta^{13}C$ of fatty acids selected to run the mixing model were the higher molecular weight of even carbons within the analysis performed (C-18 to C-24). It has been suggested by the literature the use of high molecular weight fatty acids (> 20 carbon atoms) to ensure that these molecules are more related to plant-derived organic matter (Blake et al. 2012; Upadhayay et al. 2017). However, at the time of the analysis done in a commercial laboratory (Stable Isotope Facility at UC-DAVIS), they only offered analyses of $\delta^{13}C$ for fatty acids ranging from C-14 to C-24 and no data was obtained from molecules above C-24.

2.4 Statistical Analysis

For soil apportionment, the data was analyzed using the software CSSIAR v.2.00. This software is a mixing model that works under a Bayesian framework with isotopic values for soil erosion apportionment studies. Further details of the software can be seen on the literature (Bravo-Linares et al. 2018; de los Santos-Villalobos et al. 2017). One of the key aspects of the soil apportionment calculations is the selection of the most suitable fatty acids for source discrimination (de los Santos-Villalobos et al. 2017). In this study, the fatty acid selection to perform the fingerprinting calculation was carried out by evaluating the validity of the point-in-polygon criterion (Phillips et al. 2014).

Regarding sample analyses, due to the samples were composite (reason explained in previous section) the error bars (when present) represent the analytical error.

Fig. 2 Profiles of $^{210}\text{Pb}_{\text{ex}}$ in the core sample (error bars represent the analytical error)



2.5 Core Dating

Time-average sediment accumulation rates (SARs) were estimated from excess ^{210}Pb activity concentration ($^{210}\text{Pb}_{\text{ex}}$, Bq kg⁻¹) profiles using the constant flux-constant

Table 2 Estimated age of the sediment slices by the CF-CS model

Range date	Range depth (cm)	Mid-depth (cm) and mid-year*
2008–2012	0–2	1 (2010)
2004–2008	2–4	3 (2006)
2000–2004	4–6	5 (2002)
1996–2000	6–8	7 (1998)**
1992–1996	8–10	9 (1994)
1988–1992	10–12	11 (1990)
1983–1988	12–14	13 (1985)
1979–1983	14–16	15 (1981)
1975–1979	16–18	17 (1977)
1970–1975	18–20	19 (1973)
1965–1970	20–22	21 (1968)
1960–1965	22–24	23 (1963)
1955–1960	24–26	25 (1958)*
1950–1955	26–28	27 (1953)
1945–1950	28–30	29 (1947)

*These values were used for plotting some figures presented that represents the intermediate value of the selected layer

**Segments that were not able to be used to estimate soil contribution with CSSI

sedimentation (CFCS) model (Robbins 1978). The CFCS model assumes a constant atmospheric flux of $^{210}\text{Pb}_{\text{ex}}$, so that sediments have a constant $^{210}\text{Pb}_{\text{ex}}$ at the sediment/water interface, with exponential decay over time. If sediment accumulation is the dominant process, steady-state conditions are assumed, and post-deposition mixing is negligible then the SAR (S, mm year⁻¹) can be estimated from a least-squares fit to the $^{210}\text{Pb}_{\text{ex}}$ profile using Eq. (2):

$$C_z = C_0 e^{-\lambda z/S} \tag{2}$$

where C_0 is the excess $^{210}\text{Pb}_{\text{ex}}$ activity concentration at the top slice of the core (first 2 cm) and C_z is the $^{210}\text{Pb}_{\text{ex}}$ value at depth z , λ is the decay constant for ^{210}Pb (0.03114 year⁻¹). The apparent age of sediment at a given depth is therefore an exponential function of the surface $^{210}\text{Pb}_{\text{ex}}$ value and S, assuming that sediment mixing and compaction is negligible. As described below, ^{137}Cs was present in the basal sediments of the dated core, so that confirmation of that ^{210}Pb dating using an independent FRN was not possible. In this case, the application of more complex dating models that assume temporal variation in ^{210}Pb flux and/or sediment supply (e.g., constant initial concentration (CIC) or constant rate of supply (CRS)) was not justified (Turner and Delorme, 1996). Furthermore, although soil erosion rates could be expected to vary seasonally with rainfall and river discharge, these short-term variations are not resolved at the temporal resolution of the ^{210}Pb dating (i.e., years to decades). The two regression fits to the $^{210}\text{Pb}_{\text{ex}}$ data also span several decades both before and after

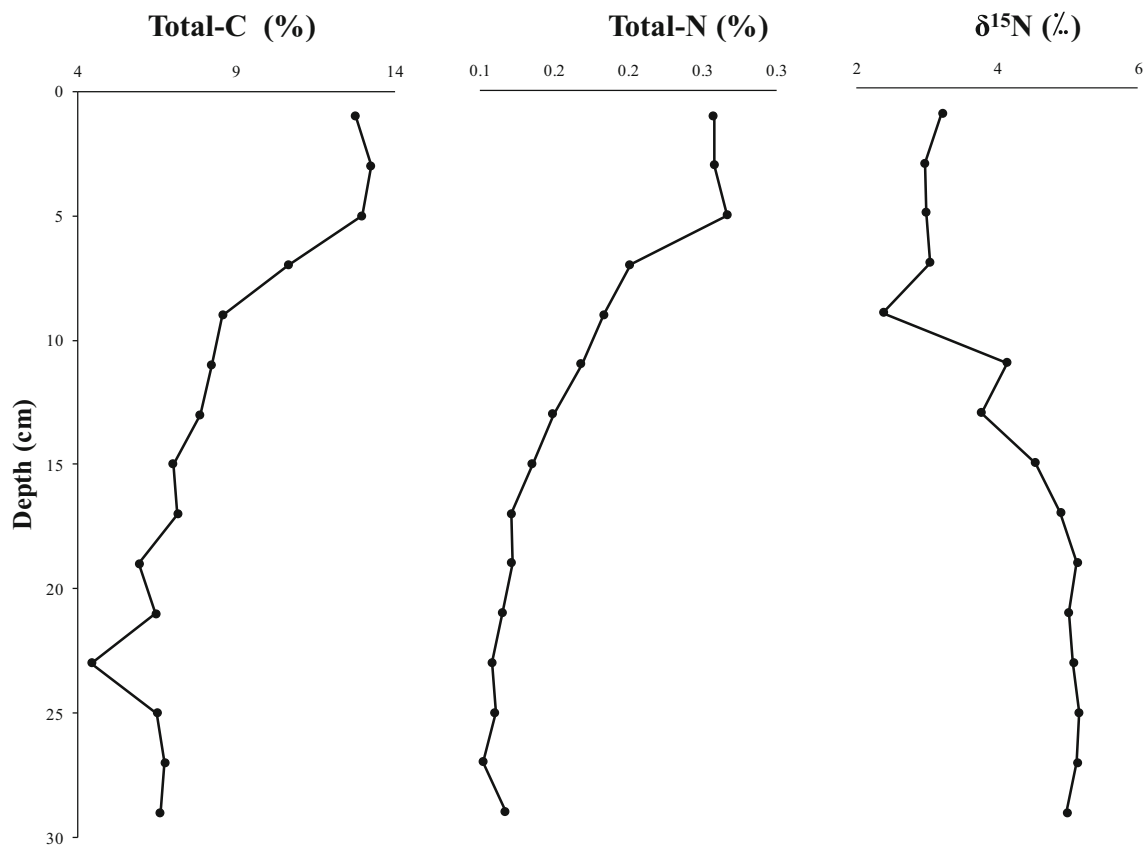


Fig. 3 Core profile for total organic carbon, nitrogen content (%), and $\delta^{15}\text{N}$ values (no replicates were done as composite samples were analyzed and axes were cut to improve the view of small changes in values)

the mid-1970s when forestry plantation was promoted by the government (Table 1), so that we are able compare changes in time-average sedimentation rates. Consequently, for these reasons, the assumption of constant sedimentation (CFCS model) is a reasonable first-order approximation of the system.

3 Results

3.1 Core Dating

The profile of $^{210}\text{Pb}_{\text{ex}}$ data is presented in Fig. 2. The results of least-square fits of the CFCS model to the Nacimiento suggested two episodes of sedimentation at 0–18 cm and 19–30 cm, with similar sediment accumulation rates of 4.8 ($r^2 = 0.75$, $P < 0.01$, $n = 9$) and 4.0 mm year^{-1} ($r^2 = 0.89$, $P < 0.005$, $n = 6$), respectively. The discontinuity in the excess $^{210}\text{Pb}_{\text{ex}}$ at 18–19-cm depth proposes a (short) interruption in sedimentation and/or change in sediment source with a less-enriched $^{210}\text{Pb}_{\text{ex}}$ content. This change in the sedimentation regime is coincident with the implementation of the executive order No. 701 that promoted the plantation of introduced trees. For example, the bottom layer could contain more eroded topsoil than the top layer. Applying these SAR values to the entire

profile yields ages of 37 years at 18-cm depth and 64 years at 30-cm depth.

^{137}Cs occurred to the base of the core (data not shown), so that independent dating using this FRN to verify the $^{210}\text{Pb}_{\text{ex}}$ was not possible (Fig. 2b). Its presence to the bottom of the core may suggest that these sediments are at least up to 60 years old. It was not possible to determine the expected peak of ^{137}Cs during the 60's as expected and to corroborate the dating with $^{210}\text{Pb}_{\text{ex}}$ (Benoit and Rozan 2001).

The calculated years according to the SAR modelling are shown in Table 2. The years estimated went back in time up to 67 years. This time was enough to cover a very important part of the history of the dramatic changes of land uses that occurred in Chile during the last 50 years.

3.2 Core Complementary Analyses

Carbon and nitrogen content (%) tended to be lower and constant the last 15 cm (Fig. 3). An increment was observed for the first top 10 cm with a marked change from the 13 cm depth upwards. During this period the forestry company reported that the catchment was harvested and planted with pines during 1990, and the use of artificial nutrients during this process is a common practice. This

Table 3 Isotopic values for calculation of source apportionment including sources after Suess correction (pine, road, buffer zone, and wheat) and mixtures (core profile)

Sample	$\delta^{13}\text{C}$ bulk	C18:0	C18:1	C18:2	C20:0	C22:0	C24:0
PINE-1	-27.5	-28.9	-30.0	-31.1	–	-30.7	-30.9
PINE-2	-27.5	-28.6	-29.9	-31.4	–	-30.5	-30.9
PINE-3	-27.3	-29.0	-30.3	-32.4	–	-30.0	-31.1
PINE-4	-27.0	-28.0	-29.7	-31.5	–	-30.7	-31.1
ROAD-1	-26.8	-29.0	-28.6	-30.3	–	-28.7	-28.8
ROAD-2	-27.0	-29.8	-31.1	-31.7	-33.1	-32.5	-32.5
ROAD-3	-27.8	-29.1	-29.7	-31.6	-28.8	-31.8	-32.1
BUFFER ZONE-1	-26.8	-29.2	-28.5	-31.2	–	-31.9	-32.1
BUFFER ZONE-2	-27.2	-28.5	-29.5	-31.3	–	-31.4	-31.8
BUFFER ZONE-3	-27.3	-28.2	-31.1	-33.2	–	-32.5	-33.3
EUCALYPTUS-1	-27.2	-30.4	-30.1	-32.2	-33.8	-31.3	-31.6
EUCALYPTUS-2	-27.5	-29.2	-29.3	-30.9	–	-30.8	-31.5
EUCALYPTUS-3	-27.4	-29.5	-29.3	-31.0	–	-31.3	-32.6
WHEAT	–	-30.3	-31.5	-31.2	-31.9	-33.2	-31.9
CORE-0002	-27.9	-28.8	-28.6	-29.0	-33.9	-32.4	-34.0
CORE-0204	-28.2	-27.0	-27.0	-28.4	-29.6	-30.9	-31.7
CORE-0406	-28.3	-26.6	-29.2	-28.4	-29.2	-29.1	-31.6
CORE-0608	-28.5	-26.5	-26.7	-26.4	–	-29.0	-31.0
CORE-0810	-28.6	-27.4	-27.4	-27.3	–	-28.7	-30.4
CORE-1012	-28.6	-27.7	-29.6	-27.2	–	-29.8	-31.6
CORE-1214	-28.6	-28.6	-26.4	-29.8	–	–	-31.4
CORE-1416	-28.5	-29.5	-27.7	-28.5	–	–	-31.4
CORE-1618	-28.3	-29.5	–	-30.4	–	-31.0	-31.9
CORE-1820	-28.4	-28.3	–	-28.2	–	–	-31.0
CORE-2022	-28.5	-28.2	-28.1	-29.3	–	–	–
CORE-2224	-28.5	-28.1	–	-31.1	–	–	-32.1
CORE-2426	-28.6	-30.7	–	–	–	-27.5	-30.2
CORE-2628	-28.7	-25.1	–	-30.9	–	–	-31.2
CORE-2830	-28.8	-27.8	-25.8	-28.7	–	–	-30.8

– no data

process can be confirmed by the lower isotopic values of $\delta^{15}\text{N}$ (from 13 cm upwards) that are an indicator of the use of artificial nitrogen containing nutrients (Hoefs 2009; Bateman and Kelly 2007) (Figure 3). Nevertheless, this difference in $\delta^{15}\text{N}$ values was not strong enough to make significant correlations with known processes (e.g., use of artificial nutrients) occurring in the catchment.

3.3 Suess Effect

The CSSI values of the $\delta^{13}\text{C}$ -FA for the core sections were corrected by the isotopic depletion value calculated from the 6th polynomial equation from Verburg (2007), and with the absolute value of 8.5‰ (obtained by the equation) of the date were the core was taken (year 2012). After this correction (Table 3), the isotopic values changed as seen in Fig. 4. The original curve presented values of bulk of $\delta^{13}\text{C}$ from -27.9‰ (top) to -27.2‰ (bottom) and after the Suess correction changed to -28.0‰ (top) to -28.8‰

(bottom). The original curve presented bulk $\delta^{13}\text{C}$ values more depleted at the surface that were closer to C3 plants angiosperms (e.g., wheat), with $\delta^{13}\text{C}$ values close to the values reported by the literature for this land use of $-32.8 \pm 2.5\text{‰}$ (Reiffarth et al. 2016; Chikaraishi and Naraoka 2006). At the surface, the values were closer to C3 plants gymnosperms (e.g., pine) with values closer to the reported in the literature of $-26.9 \pm 1.1\text{‰}$ (Reiffarth et al. 2016; Chikaraishi and Naraoka 2006).

3.4 CSSI Values

Source apportionment of the historic land uses according to the estimated date in the core samples are shown in Fig. 5. It was not possible to estimate soil proportions for core depths at 6–8 cm and 24–26 cm because the available isotopic values of these core slices did not meet the point-in-polygon criterion (Phillips et al. 2014). The kite graphs (Fig. 5) indicate the historical contributions of the five land uses during the last

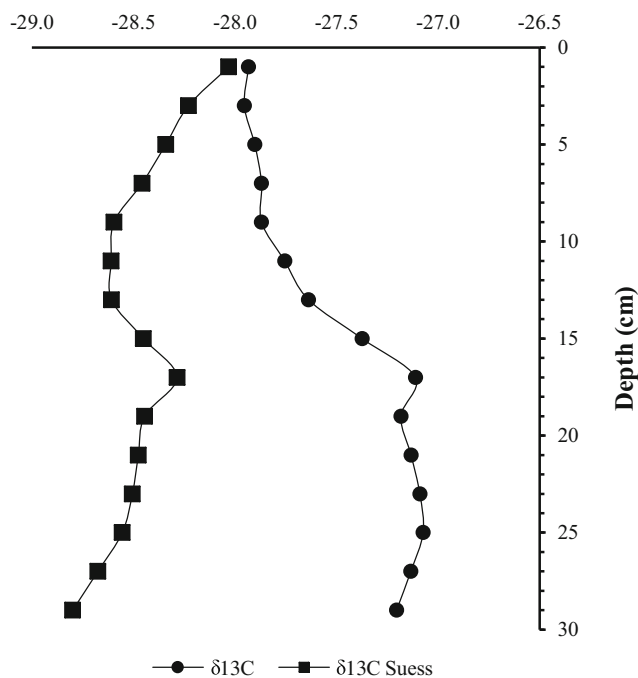


Fig. 4 Changes in the bulk $\delta^{13}\text{C}$ (‰) values (x-axis): before (circles) and after (squares) the Suess effect correction vs depth (cm)

67 years. These show that the wheat contribution was confined to the dates where historically wheat cultivation was present in the catchment (1945 to ~1974). From that date, the wheat was not planted again, and the isotopic signature of wheat gradually reduced to below detection level from 1977 onwards. This is expected, as the executive order No. 701 that promoted the plantation of exotic trees was established around this year, and made a significant change in the land use of this region (from wheat to exotic tree plantation).

On the other hand, pine became an important source of sediment following the introduction of that specie in 1963. From the soil proportion estimates (Fig. 5), the impact of sediment delivery from the pine plantation can be followed through the 1st harvesting, replanting and 2nd harvest period during 1960 and 1986, respectively. However, the results showed slight discrepancies in the dates for these actions, showing an increment in the pine signature from 1977 that denoted an impact of the bare soil being affected by erosion from the 1977 up to 1985, when the second plantation occurred and the trees matured and the sediment mobilization became lower (Schuller et al. 2013). From 1994 to 2012, the signature of pine has reduced, because the catchment has not been harvested and the canopy and pines needles provide a very good protection from erosion (Bravo-Linares et al. 2018; Doerr et al. 1998).

Regarding the eucalyptus signature, it is important to clarify that the studied catchment has not been planted with this specie. However, the neighboring catchment did. It is possible that sediment from the eucalyptus forest planted in the

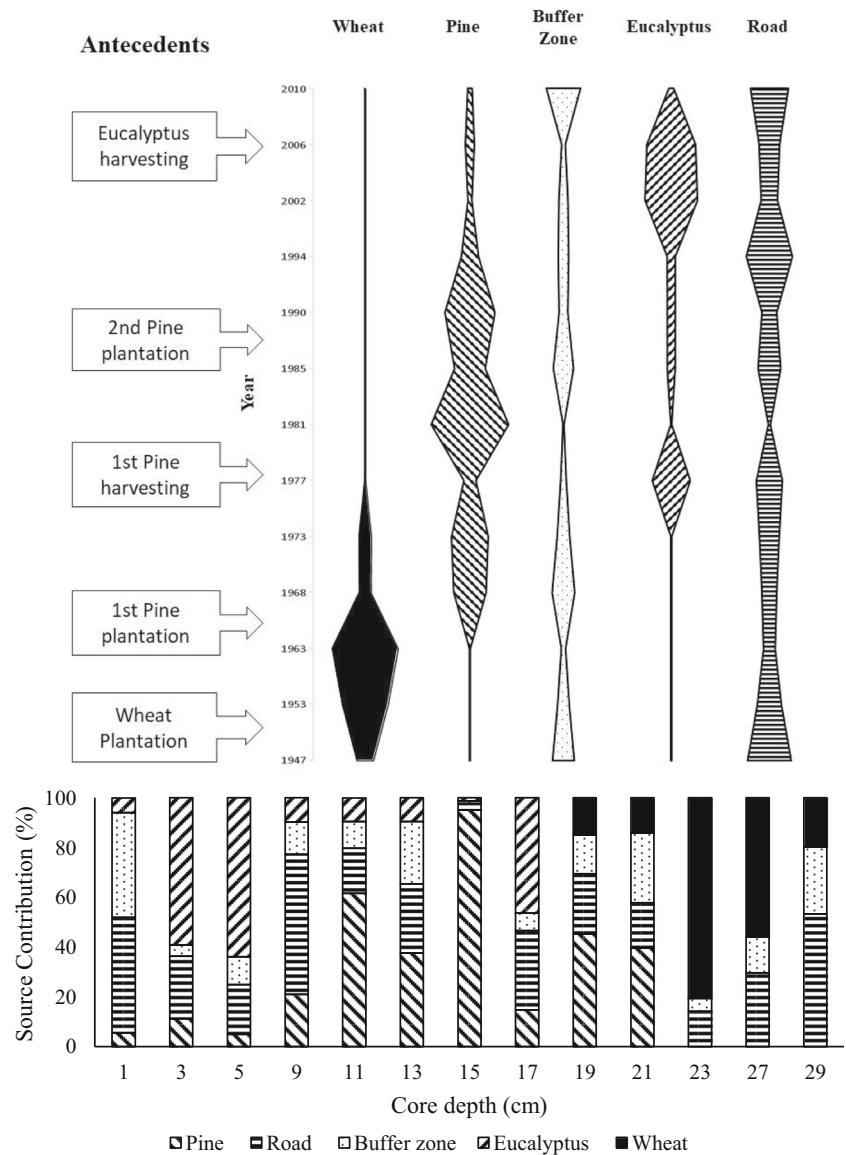
neighbor catchment has reached the stream channel where the sediment samples were taken as observed in the results (see Fig. 6).

The eucalyptus signature showed an increase in sediment delivery between 1973 and 1981, possibly due to the neighboring catchments being planted with eucalyptus, then harvested and planted again during this period. Subsequently, the eucalyptus signature became lower for 10 years to 1994 and then increased again associated with the harvesting and second planting in the neighbor catchment. The second harvesting and plantation of the paired catchments can be seen on satellites images from Google Earth (Fig. 6). These images proved evidence that the paired catchment (to the right) was harvested during 2007 to 2010 and planted again from 2010. According to this, there is a discrepancy of 3 to 6 years with the calculation and estimated dates of this study and the observed sediment delivery from this source. These discrepancies are expected as different models get different results and are estimations of the reality (Brandt et al. 2018b).

Moreover, the buffer zone (that represents the native forest that grows naturally in this catchment) remained stable during the whole period. This area is not expected to contribute much sediment as it is not meant to be affected by harvesting during the period covered by this research. Nevertheless, soil erosion was probably very high when the native forest was removed to plant wheat. As the buffer zone (native forest) in forest catchment is normally used to protect the water bodies from sediment impacts (leaving 10 m in both sides), this area traps the sediment coming from other sources (Cuevas et al. 2018). However, when storms events occur the sediment trapped can be washed out providing a delayed increase in sediment delivery from this source (Marutani et al. 1999). The same is true for earthquakes; three big earthquakes were recorded during the study period (in 1960, 1981, and 2010 with epicenters close to the study area). These episodes can increase the stream flow and, subsequently, increase the sediment delivery from the buffer zone (Schuller et al. 2013; Wang and Manga 2010). Both processes can be seen in Fig. 6, during 1960 a big earthquake and some storms affected the area and the contribution of the native forest increased from 5.2 to 28%. Similar earthquake responses occurred during 1981 from 1.1 to 25% and 2010 from 4.5 to 42.2%.

Forest roads are expected to contribute from 1960 or near dates, when the forest roads may be constructed to plant and harvest the pines trees. Roads are built by digging the soil (around 30 to 50 cm) to have access to the catchment. This source, in a contemporary point of view, can represent the land uses that were in the past. This effect can be seen during 1947 to 1963, where wheat was the main source followed by road contribution. However, the name stated by this research as a contemporary source called “roads” fits only after road building. Before that, the sediment coming from this source may represent other historical land uses that were previously

Fig. 5 Kite chart (top) and stacked bar chart (bottom) representing the historical land use soil contribution in the studied catchment considering five different land uses present during the last 67 years



present in the catchment. This may explain why roads were present in the bottom segment of the core. On the other hand, the road signature increased again after 1990, this is expected after forest stabilization (mature forest) are not prone to erosion and roads become the main source of sediment in this catchment (Bravo-Linares et al. 2018; Schuller et al. 2013).

4 Discussion

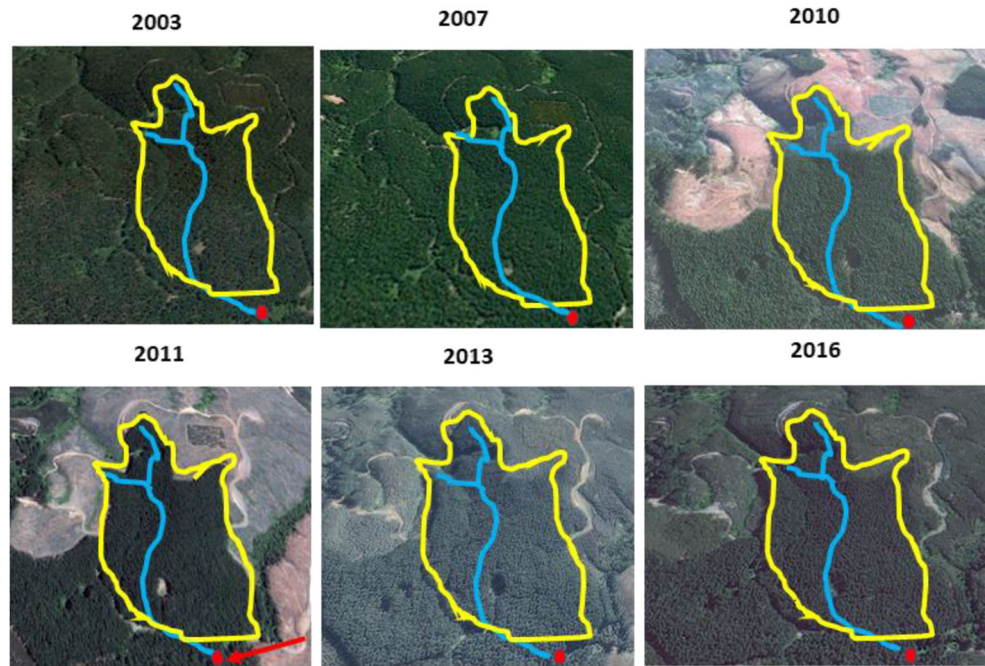
4.1 Sediment Dating

The absence of the historical ¹³⁷Cs early-1960 deposition peak has several potential explanations. Firstly, the 30-cm sediment-core length may not have been sufficient to sample the ¹³⁷Cs deposition peak. Alternatively, atmospheric deposition rates in this area of the southern hemisphere may have been

too low. It is more likely that sediments at the core site, deposited in the main stream bed, are substantially composed of eroded catchment soils and subsoils with low ¹³⁷Cs activities (i.e., rather than direct atmospheric deposition). Consequently, the ¹³⁷Cs profile reflects the soil erosion sources rather than the historical ¹³⁷Cs atmospheric deposition record (Swales et al., 2002). By contrast, a core taken by our group in an Antarctic lake (unpublished results) with similar deposition rate (5 mm year⁻¹) contained a ¹³⁷Cs peak and was used to verify the ²¹⁰Pb_{ex} dating results.

Postdepositional mobility of ¹³⁷Cs can also occur in some environments (Foster et al. 2006). Reference sites around the Nacimiento catchment showed a maximal depth of ¹³⁷Cs at 12 and 15 cm, respectively. Consequently, 30 cm core profiles were taken to ensure the presence of this chemical in the deposition area. Nevertheless, the selected deposition site may not be the most appropriate in terms of the

Fig. 6 Satellite images from Google Earth showing how the neighboring catchments planted with eucalyptus where again harvested and planted. Red dot indicates the downstream mixture and red arrow signs the influence of sediments that may be originated from the neighbor catchment



conservativeness of an undisturbed sedimentation process. However, the sample was taken in very narrow stream channel (with low flow) and in an area that somehow represents a less-disturbed part (meander). Additionally, due to this stream is not a river system, the sediment conservativeness in this system is expected to be more stable. Despite of this limitation, the relationship with the obtained results and the known antecedents of a very small catchment worked quite well as presented in the article.

Regarding the Suess effect correction, the original values (with no correction applied) were not in agreement with the antecedents recorded to the history of the land uses of the catchment. The land uses in the studied catchment (see Table 1) had a transition from angiosperms to gymnosperms, and this situation was isotopically seen when the Suess effect correction was applied to the bulk $\delta^{13}\text{C}$. The same was true for all the $\delta^{13}\text{C}$ -FA values, which were initially not able to be used to calculate the soil apportionment using contemporary sources, due to the shift in the isotopic values of the core fractions when no Suess correction was applied. This implies the importance of using this correction when a temporal assessment of source contribution is done using core samples.

4.2 Plantation Forestry and Soil Erosion

Commercial forest plantations cover a vast territory in Chile. Despite plantation forestry being a solution to past soil erosion and unsustainable land use practices (i.e., wheat plantation); inappropriate management practices have resulted in forestry plantations substantially contributing to soil erosion in upland catchments. The impacts of forest plantations on sediment

delivery and in-stream water quality during the different road building and forest-harvesting phases are important factors that need to be addressed. Sediment delivery as stated in this research can change in time according to the process involved within the catchment. Clear-cutting has been shown to cause deterioration of water quality even when a 10-m buffer zone is used. Previous research in Nacimiento catchment (comparing the pre-harvest and post-harvest situations) showed that the amount of sediment delivery after clear-cutting were three to seven times higher compared to pre-harvest conditions (Schuller et al. 2013).

Here, the combined techniques of CSSI-FRN has enabled the source apportionment different land use types to downstream sediments over a time scale of several decades (i.e., mid-1940s to 2012). This historical perspective enables the persistence of the various land use sources to soil erosion over time-scales relevant to land uses changes, climate, erosion, and cycles to be evaluated. These techniques have already shown to be useful in assessing soil erosion in forestry catchments and targeting improved management of sediment sources (Hancock and Reville 2013). However, the articles published using combined isotopic techniques are very limited. These isotopic tools can be used to assess how historical land uses have impacted an area and provide the information required to evaluate how mitigation actions have been working.

5 Conclusions

Combined isotopic techniques (compound specific stable isotopes-fallout radionuclides) allowed determination of the

proportional contribution of different land use types to sediments from the study catchment in a time scale of 67 years, and the results were similar to the historical records of the land uses in the study site.

Nevertheless, when using this combined isotopic approach, it is important to correct the data for the changes in the isotopic signatures of the sources that will change through the time, due to the isotopic changes in the $\delta^{13}\text{C}$ of the carbon dioxide (CO_2) used by the plants to synthesize organic molecules (Suess effect).

Policy making did not affect sedimentation significantly in this study site. However, it is not possible to extrapolate the same situation to all the rest of the territories that had a change from wheat to exotic trees plantations. Nevertheless, if the situation is the same, it is possible to conclude that despite of the public bill No. 701 of being a solution to a very bad land management, the sediment delivery did not change significantly, and the problem of erosion persisted through the time.

Finally, this approach is a good opportunity for land managers to evaluate how their land uses have been affecting the sediment delivery outside the catchment and to obtain better information about the off-site impacts of the erosion process.

Acknowledgments The authors thanks to the laboratory staff who analyzed the bulk $\delta^{13}\text{C}$, %C, %N, and $\delta^{15}\text{N}$ at stable isotope facility at the National Institute of Water and Atmospheric Research (NIWA) Ltd. in Wellington, New Zealand, and the compound-specific stable isotopes of fatty acids at the stable isotope facility at UC Davis, CA, USA. We also would like to acknowledge the financial support of the IAEA through the Project RLA5064 entitled “Strengthening Soil and Water Conservation Strategies at the Landscape Level by Using Innovative Radio and Stable Isotope and Related Techniques (ARCAL CXL),” to IAEA-FAO Coordinated Research Project D1.50.17: Nuclear Techniques for a Better Understanding of the Impact of Climate Change on Soil Erosion in Upland Agro-ecosystems and to Forestal Mininco to perform the study in the Nacimiento catchment.

Funding Information This project was funded by the IAEA Project RLA5064 “Strengthening Soil and Water Conservation Strategies at the Landscape Level by Using Innovative Radio and Stable Isotope and Related Techniques (ARCAL CXL)” and also by IAEA-FAO Coordinated Research Project D1.50.17: Nuclear Techniques for a Better Understanding of the Impact of Climate Change on Soil Erosion in Upland Agro-ecosystems.

Compliance with Ethical Standards

Conflict of Interest The authors declare that they have no conflict of interest.

References

- Bateman AS, Kelly SD (2007) Fertilizer nitrogen isotope signatures. *Isot Environ Health Stud* 43(3):237–247
- Benoit G, Rozan TF (2001) ^{210}Pb and ^{137}Cs dating methods in lakes: a retrospective study. *J Paleolimnol* 25(4):455–465
- Blake WH, Ficken KJ, Taylor P, Russell MA, Walling DE (2012) Tracing crop-specific sediment sources in agricultural catchments. *Geomorphology* 139:322–329
- Bonilla CA, Reyes JL, Magri A (2010) Water erosion prediction using the revised universal soil loss equation (RUSLE) in a GIS framework, Central Chile. *Chil J Agric Res* 70(1):159–169
- Brandt C, Benmansour M, Walz L, Nguyen LT, Cadisch G, Rasche F (2018a) Integrating compound-specific $\delta^{13}\text{C}$ isotopes and fallout radionuclides to retrace land use type-specific net erosion rates in a small tropical catchment exposed to intense land use change. *Geoderma* 310:53–64
- Brandt C, Dercon G, Cadisch G, Nguyen LT, Schuller P, Linares CB, Santana AC, Golosov V, Benmansour M, Amenzou N, Xinbao Z, Rasche F (2018b) Towards global applicability? Erosion source discrimination across catchments using compound-specific $\delta^{13}\text{C}$ isotopes. *Agric Ecosyst Environ* 256:114–122
- Bravo-Linares C, Schuller P, Castillo A, Ovando-Fuentealba L, Muñoz-Arcos E, Alarcón O, de los Santos-Villalobos S, Cardoso R, Muniz M, Meigikos dos Anjos R, Bustamante-Ortega R, Dercon G (2018) First use of a compound-specific stable isotope (CSSI) technique to trace sediment transport in upland forest catchments of Chile. *Sci Total Environ* 618:1114–1124
- Brunel N, Seguel O, Acevedo E (2013) Conservation tillage and water availability for wheat in the dryland of central Chile. *J Soil Sci Plant Nutr* 13:622–637
- Chikaraishi Y, Naraoka H (2006) Carbon and hydrogen isotope variation of plant biomarkers in a plant-soil system. *Chem Geol* 231(3):190–202
- Cooper RJ, Pedentchouk N, Hiscock KM, Disdle P, Krueger T, Rawlins BG (2015) Apportioning sources of organic matter in streambed sediments: an integrated molecular and compound-specific stable isotope approach. *Sci Total Environ* 520:187–197
- Cuevas JG, Little C, Lobos D, Lara A, Pino M, Acuna A (2018) Nutrient and sediment losses to streams after intervention of Eucalyptus plantations. *J Soil Sci Plant Nutr* 18:576–596
- de los Santos-Villalobos S, Bravo-Linares C, Meigikos dos Anjos R, Cardoso R, Gibbs M, Swales A, Mabit L, Dercon G (2017) The CSSIAR v.1.00 software: a new tool based on SIAR to assess soil redistribution using compound specific stable isotopes. *SoftwareX* 6:13–18
- Dercon G, Mabit L, Hancock G, Nguyen ML, Dornhofer R, Bacchi OOS, Benmansour M, Bernard C, Froehlich W, Golosov VN, Hacıyakupoglu S, Hai PS, Klik A, Li Y, Lobb DA, Onda Y, Popa N, Rafiq M, Ritchie JC, Schuller P, Shakhashiro A, Wallbrink P, Walling DE, Zapata F, Zhang X (2012) Fallout radionuclide-based techniques for assessing the impact of soil conservation measures on erosion control and soil quality: an overview of the main lessons learnt under an FAO/IAEA Coordinated Research Project. *J Environ Radioact* 107:78–85
- Doerr SH, Shakesby RA, Walsh RPD (1998) Spatial variability of soil hydrophobicity in fire-prone eucalyptus and pine forests, Portugal. *Soil Sci* 163(4):313–324
- Foster IDL, Mighall TM, Proffitt H, Walling DE, Owens PN (2006) Post-depositional ^{137}Cs mobility in the sediments of three shallow coastal lagoons. *SW England J Paleolimn* 35(4):881–895
- Gibbs MM (2008) Identifying source soils in contemporary estuarine sediments: a new compound-specific isotope method. *Estuar Coasts* 31(2):344–359
- Gysling A, Álvarez V, Soto D, Pardo E, Toledo R, Poblete P, González P, Bañados J (2016) Chilean statistical yearbook of forestry. Santiago, Chile, In I. Forestal, p 171
- Hancock GJ, Revill AT (2013) Erosion source discrimination in a rural Australian catchment using compound-specific isotope analysis (CSIA). *Hydrol Process* 27(6):923–932
- Hoefs J (2009) Stable isotope geochemistry. Springer-Verlag, Berlin Heidelberg, p 286

- Mabit L, Gibbs M, Mbaye M, Meusburger K, Toloza A, Resch C, Klik A, Swales A, Alewell C (2018) Novel application of compound specific stable isotope (CSSI) techniques to investigate on-site sediment origins across arable fields. *Geoderma* 316:19–26
- Mabit L, Meusburger K, Fulajtar E, Alewell C (2013) The usefulness of Cs-137 as a tracer for soil erosion assessment: a critical reply to Parsons and Foster (2011). *Earth Sci Rev* 127:300–307
- Marutani T, Kasai M, Reid LM, Trustrum NA (1999) Influence of storm-related sediment storage on the sediment delivery from tributary catchments in the upper Waipaoa River, New Zealand. *Earth Surf Process Landf* 24(10):881–896
- Pepin E, Carretier S, Guyot JL, Escobar F (2010) Specific suspended sediment yields of the Andean rivers of Chile and their relationship to climate, slope and vegetation. *Hydrol Sci J-J Des Sci Hydrol* 55(7):1190–1205
- Phillips DL, Inger R, Bearhop S, Jackson AL, Moore JW, Parnell AC, Semmens BX, Ward EJ (2014) Best practices for use of stable isotope mixing models in food-web studies. *Can J Zool* 92(10):823–835
- Reiffarth DG, Petticrew EL, Owens PN, Lobb DA (2016) Sources of variability in fatty acid (FA) biomarkers in the application of compound-specific stable isotopes (CSSIs) to soil and sediment fingerprinting and tracing: a review. *Sci Total Environ* 565:8–27
- Robbins JA (1978) Geochemical and geophysical applications of radioactive lead. In: Nriagu JO (ed) *Biogeochemistry of lead in the environment*. Elsevier, Amsterdam, pp 285–393
- Schuller P, Walling DE, Iroume A, Quilodran C, Castillo A, Navas A (2013) Using Cs-137 and Pb-210(ex) and other sediment source fingerprints to document suspended sediment sources in small forested catchments in south-central Chile. *J Environ Radioact* 124:147–159
- Smith HG, Blake WH (2014) Sediment fingerprinting in agricultural catchments: a critical re-examination of source discrimination and data corrections. *Geomorphology* 204:177–191
- Swales A, Williamson RB, Van Dam LF, Stroud MJ, McGlone MS (2002) Reconstruction of urban stormwater contamination of an estuary using catchment history and sediment profile dating. *Estuaries* 25:43–56
- Taylor A, Blake WH, Smith HG, Mabit L, Keith-Roach MJ (2013) Assumptions and challenges in the use of fallout beryllium-7 as a soil and sediment tracer in river basins. *Earth Sci Rev* 126:85–95
- Tolorza V, Carretier S, Andermann C, Ortega-Culaciati F, Pinto L, Mardones M (2014) Contrasting mountain and piedmont dynamics of sediment discharge associated with groundwater storage variation in the Biobio River. *J Geophys Res-Earth Surf* 119(12):2730–2753
- Turner LJ, Delorme LD (1996) Assessment of Pb-210 data from Canadian lakes using the CIC and CRS models. *Environ. Geol.* 28:78–87
- Upadhyay HR, Bodé S, Griepentrog M, Huygens D, Bajracharya RM, Blake WH, Dercon G, Mabit L, Gibbs M, Semmens BX, Stock BC, Cornelis W, Boeckx P (2017) Methodological perspectives on the application of compound-specific stable isotope fingerprinting for sediment source apportionment. *J Soils Sediments* 17(6):1537–1553
- Verburg P (2007) The need to correct for the Suess effect in the application of delta C-13 in sediment of autotrophic Lake Tanganyika, as a productivity proxy in the Anthropocene. *J Paleolimnol* 37(4):591–602
- Wang CY, Manga M (2010) Hydrologic responses to earthquakes and a general metric. *Geofluids* 10(1–2):206–216

Publisher's note Springer Nature remains neutral with regard to jurisdictional claims in published maps and institutional affiliations.